
SAMPLE BASED EXPLANATIONS VIA GENERALIZED REPRESENTERS

A PREPRINT

Che-Ping Tsai
Machine Learning Department
Carnegie Mellon University
chepingt@andrew.cmu.edu

Chih-Kuan Yeh
Google Deepmind *
jason6582@gmail.com

Pradeep Ravikumar
Machine Learning Department
Carnegie Mellon University
pradeepr@cs.cmu.edu

ABSTRACT

We propose a general class of sample based explanations of machine learning models, which we term *generalized representers*. To measure the effect of a training sample on a model's test prediction, generalized representers use two components: a *global sample importance* that quantifies the importance of the training point to the model and is invariant to test samples, and a *local sample importance* that measures similarity between the training sample and the test point with a kernel. A key contribution of the paper is to show that generalized representers are the only class of sample based explanations satisfying a natural set of axiomatic properties. We discuss approaches to extract global importances given a kernel, and also natural choices of kernels given modern non-linear models. As we show, many popular existing sample based explanations could be cast as generalized representers with particular choices of kernels and approaches to extract global importances. Additionally, we conduct empirical comparisons of different generalized representers on two image and two text classification datasets.

1 Introduction

As machine learning becomes increasingly integrated into various aspects of human life, the demand for understanding, interpreting, and explaining the decisions made by complex AI and machine learning models has grown. Consequently, numerous approaches have been proposed in the field of Explainable AI (XAI). Feature based explanations interpret models by identifying the most relevant input features [1, 2, 3, 4], while sample based explanations do so via the most relevant training samples [5, 6, 7, 8]. Although different methods emphasize different aspects of the model, some may even have conflicting philosophies [9]. To address this issue, there have been growing calls within the XAI community for more objective or normative approaches [10, 11, 12], which could help align XAI techniques more effectively with human needs.

One of the most straightforward approaches to assess the effectiveness of explanations is by evaluating their utility in downstream applications [13, 14]. However, such evaluations can be costly, particularly during the development stages of explanations, as they often necessitate the involvement of real human users. As a result, a well-grounded, axiom-based evaluation can be beneficial for designing and selecting explanations for implementation. Axioms can be viewed as theoretical constraints that dictate how explanations should behave in response to specific inputs. A notable example is the Shapley value [15], which originated in cooperative game theory and has gained popularity in XAI due to its appealing axiomatic properties. Nonetheless, while axiomatic approaches have been widely applied in identifying significant features [4, 16, 17], feature interactions [18, 19], and high-level concepts [20], they have not been extensively discussed in sample based explanations.

In this work, we propose a set of desirable axioms for sample based explanations. We then show that any sample based attributions that satisfy (a subset of) these axioms are necessarily the product of two components: a *global sample importance*, and a *local sample importance* that is a kernel similarity between a training sample and the test point. We term the explanations in this form *generalized representers*.

*Work done in Carnegie Mellon University.

We note that the efficiency axiom (detailed in the sequel) can only be satisfied if the model function lies in the RKHS subspace spanned by the training kernel representers, which is indeed typically the case. Otherwise, we could ask for the smallest error in satisfying the efficiency axiom which can be cast as an RKHS regression problem. Thus, given a kernel, extracting global importances can be cast as solving an RKHS regression problem, by recourse to RKHS representer theorems [21]. We additionally also propose *tracking representers* that scalably compute the global importance by tracking kernel gradient descent trajectories.

The class of generalized representers allow for the user to specify a natural kernel given the model they wish to explain, perhaps drawn from domain knowledge. We discuss some natural automated choices given modern non-linear models. Specifically, we discuss the kernel with feature maps specified by last-layer embeddings, neural tangent kernels [22], and influence function kernels [5]. Many existing sample-based explanation methods such as representer point selection [7], and influence functions [5] can be viewed as specific instances of the broad class of generalized representers. As we show, TracIn [6] could be viewed as a natural extension of generalized representers that uses multiple kernels, and computes multiple corresponding global and local importances. We empirically compare different choices of generalized representers for neural networks on two image and two text classification datasets.

1.1 Related work

Axiomatic attribution in XAI: The most common line of work that incorporates axioms in the design of explanations is the family of Shapley values [15], that originates from cooperative game theory. This line of work first tackles the attribution problem by converting it into a set value function and then applying the Shapley value. The Shapley value is widely used in feature-based explanations [4, 16, 23], feature-interaction explanations [18, 19], concept-based explanations [20] and sample-based explanations [8].

We note that the axiomatic framework for sample-based explanations in data Shapley [8] has distinct purposes and interpretations to ours. Generalized representers assess the significance of training samples with respect to a specific test sample’s prediction. In contrast, data Shapley assesses training sample importance via training loss and can be directly adapted to original Shapley value axioms. Consequently, while there are shared axiomatic principles between the two frameworks, the generalized representers require a different approach due to their additional focus on a specific test sample. We will delve into a detailed comparison of these distinctions in Section 3.

Sample based explanations: Existing sample-based explanation approaches can be separated into retraining-based and gradient-based approaches [24]. Retraining-based approaches are based on the measurement of the difference between a model prediction with and without a group of training samples [25, 26, 27, 28, 29, 30, 31, 32, 33, 8, 34]. Gradient-based methods estimate data influence based on similarities between gradients. The majority of methods build upon the three theoretical frameworks, namely: (1) Representer theorems [7, 35, 36, 37], (2) Hessian-based influence functions [5, 38, 39, 40, 41, 42, 43, 44, 45], and (3) Decomposing the training loss trajectory [6, 46, 47, 48]. In this work, we show that most gradient-based methods can be viewed as generalized representers.

2 Problem Definition

We consider the task of explaining a supervised machine learning model $f : \mathbb{R}^d \mapsto \mathbb{R}$, given inputs $\mathbf{x} \in \mathbb{R}^d$, where d is the input dimension.² We are interested in explaining such models $f(\cdot)$ in terms of the training points $\mathcal{D} := \{(\mathbf{x}_i, y_i)\}_{i=1}^n$ with each training sample $(\mathbf{x}_i, y_i) \in \mathbb{R}^d \times \mathbb{R}$. We denote a *sample explanation functional* $\phi_{\mathcal{D}} : \mathcal{F} \times \mathcal{D} \times \mathbb{R}^d \mapsto \mathbb{R}^n$, as a mapping that takes a real-valued model $f \in \mathcal{F}$, training data points \mathcal{D} , and an arbitrary test data point $\mathbf{x} \in \mathbb{R}^d$ as input, and outputs a vector of explanation weights $[\phi_{\mathcal{D}}(f, (\mathbf{x}_1, y_1), \mathbf{x}), \dots, \phi_{\mathcal{D}}(f, (\mathbf{x}_n, y_n), \mathbf{x})] \in \mathbb{R}^n$ with each value corresponding to an importance score of each training sample to the test point. In the sequel, we will suppress the explicit dependence on the entire set of training points in the notation for the explanation functional and the dependence on the training label y_i . Also, to make clear that the first data point argument is the training sample, and the second is the test sample, we will use $\phi(f, \mathbf{x}_i \rightarrow \mathbf{x}) \in \mathbb{R}$ to denote the sample explanation weight for \mathbf{x}_i to explain the prediction of the model $f(\cdot)$ for the test point \mathbf{x} .

3 Axioms for Sample based Explanations

In this section, we begin by presenting a collection of axioms that describe various desirable characteristics of sample based explanations.

²Note that we assume a single-dimensional output for notational convenience. In the appendix, we show that our development can be extended to vector-valued outputs by using vector-output kernel functions.

Definition 1 (Efficiency Axiom). *For any model f , and test point $x \in \mathbb{R}^d$, a sample based explanation $\phi(\cdot)$ satisfies the efficiency axiom iff:*

$$\sum_{i=1}^n \phi(f, \mathbf{x}_i \rightarrow \mathbf{x}) = f(\mathbf{x}).$$

The efficiency axiom entails that the sum of the attributions to each training sample together adds up to the model prediction at the test point. This is a natural counterpart of the efficiency axioms used in the Shapley values [49].

Definition 2 (Self-Explanation Axiom). *A sample based explanation $\phi(\cdot)$ satisfies the self-explanation axiom iff there exists any training point \mathbf{x}_i having no effect on itself, i.e. $\phi(f, \mathbf{x}_i \rightarrow \mathbf{x}_i) = 0$, the training point should not impact any other points, i.e. $\phi(f, \mathbf{x}_i \rightarrow \mathbf{x}) = 0$ for all $\mathbf{x} \in \mathbb{R}^d$.*

The self-explanation axiom states that if the label y_i does not even have an impact on the model's prediction for \mathbf{x}_i , it should not impact other test predictions. This axiom shares a similar intuition as the dummy axiom in the Shapley values [15] since both axioms dictate that explanations should be zero if a training sample has no impact on the model. However, the self-explanation axiom requires a different theoretical treatments due to the additional focus in generalized representers of explaining a model prediction on a particular test sample.

Definition 3 (Symmetric Zero Axiom). *A sample explanation $\phi(\cdot)$ satisfies the symmetric zero axiom iff any two training points $\mathbf{x}_i, \mathbf{x}_j$ such that if $\phi(f, \mathbf{x}_i \rightarrow \mathbf{x}_i) \neq 0$ and $\phi(f, \mathbf{x}_j \rightarrow \mathbf{x}_j) \neq 0$, then*

$$\phi(f, \mathbf{x}_i \rightarrow \mathbf{x}_j) = 0 \implies \phi(f, \mathbf{x}_j \rightarrow \mathbf{x}_i) = 0.$$

The symmetric-zero axiom underscores the bidirectional nature of "orthogonality". It emphasizes that if a sample has no impact on another sample, this lack of correlation is mutual and implies that they are orthogonal.

Definition 4 (Symmetric Cycle Axiom). *A sample explanation $\phi(\cdot)$ satisfies the symmetric cycle axiom iff for any set of training points $\mathbf{x}_{t_1}, \dots, \mathbf{x}_{t_k}$, with possible duplicates, and $\mathbf{x}_{t_{k+1}} = \mathbf{x}_{t_1}$, it holds that:*

$$\prod_{i=1}^k \phi(f, \mathbf{x}_{t_i} \rightarrow \mathbf{x}_{t_{i+1}}) = \prod_{i=1}^k \phi(f, \mathbf{x}_{t_{i+1}} \rightarrow \mathbf{x}_{t_i}).$$

Let us first consider the vacuous case of two points: $\mathbf{x}_1, \mathbf{x}_2$, for which the axiom is the tautology that: $\phi(f, \mathbf{x}_1 \rightarrow \mathbf{x}_2)\phi(f, \mathbf{x}_2 \rightarrow \mathbf{x}_1) = \phi(f, \mathbf{x}_2 \rightarrow \mathbf{x}_1)\phi(f, \mathbf{x}_1 \rightarrow \mathbf{x}_2)$. Let us next look at the case with three points: $\mathbf{x}_1, \mathbf{x}_2, \mathbf{x}_3$, for which the axiom entails:

$$\phi(f, \mathbf{x}_1 \rightarrow \mathbf{x}_2)\phi(f, \mathbf{x}_2 \rightarrow \mathbf{x}_3)\phi(f, \mathbf{x}_3 \rightarrow \mathbf{x}_1) = \phi(f, \mathbf{x}_3 \rightarrow \mathbf{x}_2)\phi(f, \mathbf{x}_2 \rightarrow \mathbf{x}_1)\phi(f, \mathbf{x}_1 \rightarrow \mathbf{x}_3).$$

It can be seen that this is a generalization of simply requiring that the explanations be symmetric as in the symmetry axiom in the Shapley values. In fact, the unique explanation satisfying this and other listed axioms is in general not symmetric. The axiom could also be viewed as a conservation or path independence law, in that the flow of explanation based information from a point \mathbf{x}_i to itself in a cycle is invariant to the path taken.

Definition 5 (Continuity Axiom). *A sample based explanation $\phi(\cdot)$ satisfies the continuity axiom iff it is continuous wrt the test data point \mathbf{x} , for any fixed training point \mathbf{x}_i :*

$$\lim_{\mathbf{x}' \rightarrow \mathbf{x}} \phi(f, \mathbf{x}_i \rightarrow \mathbf{x}') = \phi(f, \mathbf{x}_i \rightarrow \mathbf{x}).$$

Such continuity is a minimal requirement on the regularity of the explanation functional, and which ensures that infinitesimal changes to the test point would not incur large changes to the explanation functional.

Definition 6 (Irreducibility Axiom). *A sample explanation $\phi(\cdot)$ satisfies the irreducibility axiom iff for any number of training points $\mathbf{x}_1, \dots, \mathbf{x}_k$,*

$$\det \begin{pmatrix} \phi(f, \mathbf{x}_1, \mathbf{x}_1) & \phi(f, \mathbf{x}_1, \mathbf{x}_2) & \dots & \phi(f, \mathbf{x}_1, \mathbf{x}_k) \\ \phi(f, \mathbf{x}_2, \mathbf{x}_1) & \phi(f, \mathbf{x}_2, \mathbf{x}_2) & \dots & \phi(f, \mathbf{x}_2, \mathbf{x}_k) \\ \dots & \dots & \dots & \dots \\ \phi(f, \mathbf{x}_k, \mathbf{x}_1) & \phi(f, \mathbf{x}_k, \mathbf{x}_2) & \dots & \phi(f, \mathbf{x}_k, \mathbf{x}_k) \end{pmatrix} \geq 0.$$

A sufficient condition for an explanation $\phi(\cdot)$ to satisfy the irreducibility axiom is for

$$|\phi(f, \mathbf{x}_i \rightarrow \mathbf{x}_i)| > \sum_{j \neq i} |\phi(f, \mathbf{x}_i \rightarrow \mathbf{x}_j)|, \quad (1)$$

since this makes the matrix above strictly diagonally dominant, and since the diagonal entries are non-negative, by the Gershgorin circle theorem, the eigenvalues are all non-negative as well, so that the determinant in turn is non-negative.

The continuity and irreducibility axiom primarily serves a function-analytic purpose by providing sufficient and necessary conditions of a kernel being a Mercer kernel, which requires that the kernel function be continuous and positive semi-definite.

We are now ready to investigate the class of explanations that satisfy the axioms introduced above.

Theorem 7. *An explanation functional $\phi(f, \cdot, \cdot)$ satisfies the continuity, self-explanation, symmetric zero, symmetric cycle, and irreducibility axioms for any training samples \mathcal{D} containing n training samples $(\mathbf{x}_i, y_i) \in \mathbb{R}^d \times \mathbb{R}$ for all $i \in [n]$ iff*

$$\phi(f, \mathbf{x}_i \rightarrow \mathbf{x}) = \alpha_i K(\mathbf{x}_i, \mathbf{x}) \quad \forall i \in [n], \quad (2)$$

for some $\alpha \in \mathbb{R}^n$ and some continuous positive-definite kernel $K : \mathbb{R}^d \times \mathbb{R}^d \mapsto \mathbb{R}$.

This suggests that a sample explanation $\phi(f, \mathbf{x}_i \rightarrow \mathbf{x}) = \alpha_i K(\mathbf{x}_i, \mathbf{x})$ has two components: a weight α_i associated with just the training point \mathbf{x}_i independent of test points, and a similarity $K(\mathbf{x}_i, \mathbf{x})$ between the training and test points specified by a Mercer kernel. Following Yeh et al. [7], we term the first component the *global importance* of the training sample \mathbf{x}_i and the second component the *local importance* that measures similarities between training and test samples.

Once we couple this observation together with the efficiency axiom, one explanation that satisfies these properties is:

$$f(\mathbf{x}) = \sum_{j=1}^n \phi(f, \mathbf{x}_j \rightarrow \mathbf{x}) = \sum_{j=1}^n \alpha_j K(\mathbf{x}_j, \mathbf{x}), \text{ for any } x \in \mathbb{R}^p. \quad (3)$$

This can be seen to hold only if the target function f lies in the RKHS subspace spanned by the kernel evaluations of training points. When this is not necessarily the case, then the efficiency axiom (where the sum of training sample importances equals the function value) exactly, cannot be satisfied exactly. We can however satisfy the efficiency axiom approximately with the approximation error arising from projecting the target function f onto the RKHS subspace spanned by training representers.

This thus provides a very simple and natural framework for specifying sample explanations: (1) specify a Mercer kernel $K(\cdot, \cdot)$ so that the target function can be well approximated by the corresponding kernel machine, and (2) project the given model onto the RKHS subspace spanned by kernel evaluations on the training points. Each of the sample explanation weights then has a natural specification in terms of global importance associated with each training point (arising from the projection of the function onto the RKHS subspace, which naturally does not depend on any test points), as well as a localized component that is precisely the kernel similarity between the training and test points.

4 Deriving Global Importance Given Kernel Functions

The previous section showed that the class of sample explanations that satisfy a set of key axioms naturally correspond to an RKHS subspace. Thus, all one needs, in order to specify the sample explanations, is to specify a Mercer kernel function K and solve for the corresponding global importance weights α . In this section, we focus on the latter problem, and present three methods to compute the global importance weights given some kernel K .

4.1 Method 1: Projecting Target Function onto RKHS Subspace

The first method is to project the target function onto the RKHS subspace spanned by kernel evaluations on the training points. Given the target function f , loss function $\mathcal{L} : \mathbb{R} \times \mathbb{R} \mapsto \mathbb{R}$ and training dataset $\mathcal{D} = \{(\mathbf{x}_i, y_i)\}_{i=1}^n$ (potentially, though not necessarily used to train f), and a user-specified Mercer kernel K , our goal is to find a projection \hat{f}_K of the target model onto the RKHS subspace defined by $\mathcal{H}_n = \text{span}(\{K(\mathbf{x}_i, \cdot)\}_{i=1}^n)$. To accomplish this, we formulate it as a RKHS regression problem:

$$\hat{f}_K = \underset{f_K \in \mathcal{H}_K}{\operatorname{argmin}} \left\{ \frac{1}{n} \sum_{i=1}^n \mathcal{L}(f_K(\mathbf{x}_i), f(\mathbf{x}_i)) + \frac{\lambda}{2} \|f_K\|_{\mathcal{H}_K}^2 \right\}, \quad (4)$$

where \mathcal{H}_K as the RKHS defined by kernel K , $\|\cdot\|_{\mathcal{H}_K} : \mathcal{H}_K \mapsto \mathbb{R}$ is the RKHS norm, and λ is a regularization parameter that controls the faithfulness and complexity of the function \hat{f}_K . The loss function \mathcal{L} can be chosen as the objective function used to train the target function f to closely emulate the behavior of target function f and its dependence on the training samples \mathcal{D} . By the representer theorem [21], the regularization term $\|f_K\|_{\mathcal{H}_K}^2$ added here ensures that the solution lies in the RKHS subspace \mathcal{H}_n spanned by kernel evaluations. Indeed, by the representer

theorem [21], the minimizer of Eqn.(4) can be represented as $\hat{f}_K(\cdot) = \sum_{i=1}^n \alpha_i K(\mathbf{x}_i, \cdot)$ for some $\alpha \in \mathbb{R}^n$, which allows us to reparameterize Eqn.(4):

$$\hat{\alpha} = \operatorname{argmin}_{\alpha \in \mathbb{R}^n} \left\{ \frac{1}{n} \sum_{i=1}^n \mathcal{L} \left(\sum_{j=1}^n \alpha_j K(\mathbf{x}_i, \mathbf{x}_j), f(\mathbf{x}_i) \right) + \frac{\lambda}{2} \alpha^\top \mathbf{K} \alpha \right\}, \quad (5)$$

where $\mathbf{K} \in \mathbb{R}^{n \times n}$ is the kernel gram matrix defined as $K_{ij} = K(\mathbf{x}_i, \mathbf{x}_j)$ for $i, j \in [n]$, and we use the fact that $\|f_K\|_{\mathcal{H}_K} = \langle \sum_{i=1}^n \alpha_i K(\mathbf{x}_i, \cdot), \sum_{i=1}^n \alpha_i K(\cdot, \mathbf{x}_i) \rangle^{\frac{1}{2}} = \sqrt{\alpha^\top \mathbf{K} \alpha}$. By solving the first-order optimality condition, the global importance α must be in the following form:

Proposition 8. (Surrogate derivative) *The minimizer of Eqn.(4) can be represented as $\hat{f}_K = \sum_{i=1}^n \hat{\alpha}_i K(\mathbf{x}_i, \cdot)$, where*

$$\hat{\alpha} \in \{\alpha^* + v \mid v \in \operatorname{null}(\mathbf{K})\} \text{ and } \alpha_i^* = -\frac{1}{n\lambda} \frac{\partial \mathcal{L}(\hat{f}_K(\mathbf{x}_i), f(\mathbf{x}_i))}{\partial \hat{f}_K(\mathbf{x}_i)}, \quad \forall i \in [n]. \quad (6)$$

We call α_i^* the surrogate derivative since it is the derivative of the loss function with respect to the surrogate function prediction.

α_i^* can be interpreted as the measure of how sensitive $\hat{f}_K(\mathbf{x}_i)$ is to changes in the loss function. Although the global importance α solved via Eqn.(5) may not be unique as indicated by the above results, the following proposition ensures that all $\hat{\alpha} \in \{\alpha^* + v \mid v \in \operatorname{null}(\mathbf{K})\}$ result in the same surrogate function $\hat{f}_K = \sum_{i=1}^n \alpha_i^* K(\mathbf{x}_i, \cdot)$.

Proposition 9. *For any $v \in \operatorname{null}(\mathbf{K})$, the function $f_v = \sum_{i=1}^n v_i K(\mathbf{x}_i, \cdot)$ specified by the span of kernel evaluations with weights v is a zero function, such that $f_v(\mathbf{x}) = 0$ for all $\mathbf{x} \in \mathbb{R}^d$.*

The proposition posits that adding any $v \in \operatorname{null}(\mathbf{K})$ to α^* has no effect on the function \hat{f}_K . Therefore, we use α^* to represent the global importance as it captures the sensitivity of the loss function to the prediction of the surrogate function.

4.2 Method 2: Approximation Using the Target Function

Given the derivation of global importance weights α^* in Eqn.(6), we next consider a variant replacing the surrogate function prediction $\hat{f}_K(\mathbf{x}_i)$ with the target function prediction $f(\mathbf{x}_i)$:

Definition 10 (Target derivative). *The global importance computed with derivatives of the loss function with respect to the target function prediction is defined as:*

$$\alpha_i^* = -\frac{\partial \mathcal{L}(f(x_i), y_i)}{\partial f(x_i)}, \quad \forall i \in [n], \quad (7)$$

where $\mathcal{L}(\cdot, \cdot)$ is the loss function used to train the target function.

A crucial advantage of this variant is that we no longer need solve for an RKHS regression problem. There are several reasons why this approximation is reasonable. Firstly, the loss function in Eqn.(4) encourages the surrogate function to produce similar outputs as the target function, so that $\hat{f}_K(\mathbf{x}_i)$ is approximately equal to $f(x_i)$. Secondly, when the target function exhibits low training error, which is often the case for overparameterized neural networks that are typically in an interpolation regime, we can assume that $f(x_i)$ is close to y_i . Consequently, the target derivative can serve as an approximation of the surrogate derivative in Eqn.(6). As we will show below, the influence function approach [5] is indeed as the product between the target derivative and the influence function kernel.

4.3 Method 3: Tracking Gradient Descent Trajectories

Here, we propose a more scalable variant we term *tracking representers* that accumulates changes in the global importance during kernel gradient descent updates when solving Eqn.(4). Let $\Phi: \mathbb{R}^d \mapsto \mathcal{H}$ be a feature map corresponding to the kernel K , so that $K(\mathbf{x}, \mathbf{x}') = \langle \Phi(\mathbf{x}), \Phi(\mathbf{x}') \rangle$. We can then cast any function in the RKHS as $f_K(\mathbf{x}) = \langle \theta, \Phi(\mathbf{x}) \rangle$ for some parameter $\theta \in \mathcal{H}$. Suppose we solve the unregularized projection problem in Eqn.(4) via stochastic gradient descent updates on the parameter θ : $\theta^{(t)} = \theta^{(t-1)} - \frac{\eta^{(t)}}{|B^{(t)}|} \sum_{i \in B^{(t)}} \nabla_{\theta} \mathcal{L}(f_{\theta}(\mathbf{x}_i), f(\mathbf{x}_i)) \Phi(\mathbf{x}_i)|_{\theta=\theta^{(t-1)}}$, where we use $B^{(t)}$ and $\eta^{(t)}$ to denote the minibatch and the learning rate. The corresponding updates to the function is then given by “kernel gradient descent” updates: $f_K^{(t)}(\mathbf{x}) = f_K^{(t-1)}(\mathbf{x}) - \alpha_{it} K(\mathbf{x}_i, \mathbf{x})$, where $\alpha_{it} = \frac{\eta^{(t)}}{|B^{(t)}|} \sum_{i \in B^{(t)}} \frac{\partial \mathcal{L}(f_K^{(t-1)}(\mathbf{x}_i), f(\mathbf{x}_i))}{\partial f_K^{(t-1)}(\mathbf{x}_i)}$.

The function at step T can then be represented as:

$$f_K^{(T)}(\mathbf{x}) = \sum_{i=1}^n \alpha_i^{(T)} K(\mathbf{x}_i, \mathbf{x}) + f_K^{(0)}(\mathbf{x}) \text{ with } \alpha_i^{(T)} = -\sum_{t: i \in B^{(t)}} \frac{\eta^{(t)}}{|B^{(t)}|} \frac{\partial \mathcal{L}(f_K^{(t-1)}(\mathbf{x}_i), f(\mathbf{x}_i))}{\partial f_K^{(t-1)}(\mathbf{x}_i)}. \quad (8)$$

Definition 11 (Tracking representers). *Given a finite set of steps T , we term the global importance weights obtained via tracking kernel gradient descent as tracking representers:*

$$\alpha_i^* = - \sum_{t \in [T]: i \in B^{(t)}} \frac{\eta^{(t)}}{|B^{(t)}|} \frac{\partial \mathcal{L}(f_K^{(t-1)}(\mathbf{x}_i), f(\mathbf{x}_i))}{\partial f_K^{(t-1)}(\mathbf{x}_i)}. \quad (9)$$

We note that one can draw from standard correspondences between gradient descent with finite stopping and ridge regularization (e.g. [50]), to in turn relate the iterates of the kernel gradient descent updates for any finite stopping at T iterations to regularized RKHS regression solutions for some penalty λ . The above procedure thus provides a potentially scalable approach to compute the corresponding global importances: in order to calculate the global importance $\alpha_i^{(T)}$, we need to simply monitor the evolution of $\alpha_i^{(t)}$ when the sample \mathbf{x}_i is utilized at iteration t . In our experiment, we use the following relaxation for further speed up:

$$\alpha_i^* = - \sum_{t \in [T]: i \in B^{(t)}} \frac{\eta^{(t)}}{|B^{(t)}|} \frac{\partial \mathcal{L}(f^{(t-1)}(\mathbf{x}_i), y_i)}{\partial f^{(t-1)}(\mathbf{x}_i)}, \quad (10)$$

where we assume the target model is trained with (stochastic) gradient descent, $f^{(t)}(\mathbf{x}_i)$ denotes the target model at t^{th} iteration during training, and $B^{(t)}$ and $\eta^{(t)}$ are the corresponding mini-batch and learning rate. Similar to the intuition of replacing the surrogate derivative with to target derivative, we track the target model’s training trajectory directly instead of solving Eqn.(4) with kernel gradient descent.

5 Choice of Kernels for Generalized Representers

Previously, we discussed approaches for deriving global importance given user-specified kernels, which can in general be specified by domain knowledge relating to the model and the application domain. In this section, we discuss natural choices of kernels for modern non-linear models. Moreover, we show that existing sample based explanation methods such as representer points [7] and influence functions [5] could be viewed as making particular choices of kernels when computing general representers. We also discuss TracIn [6] as a natural extension of our framework to multiple rather than a single kernel.

5.1 Kernel 1: Penultimate-layer Embeddings

A common method for extracting a random feature map from a neural network is to use the embeddings of its penultimate layer [7, 51, 52]. Let $\Phi_{\Theta_1} : \mathbb{R}^d \mapsto \mathbb{R}^\ell$ denote the mapping from the input to the second last layer. The target model f can be represented as

$$f(\mathbf{x}) = \Phi_{\Theta_1}(\mathbf{x})^\top \Theta_2, \quad (11)$$

where $\Theta_2 \in \mathbb{R}^\ell$ is the weight matrix of the last layer. That is, we treat the deep neural network as a linear machine on top of a learned feature map. The kernel function is then defined as $K_{LL}(\mathbf{x}, \mathbf{z}) = \langle \Phi_{\Theta_1}(\mathbf{x}), \Phi_{\Theta_1}(\mathbf{z}) \rangle, \forall \mathbf{x}, \mathbf{z} \in \mathbb{R}^d$. This is the case with most deep neural network architectures, where the feature map Φ_{Θ_1} is specified via deep compositions of parameterized layers that take the form of fully connected layers, convolutional layers, or attention layers among others. While the last-layer weight matrix Θ_2 may not lie in the span of $\{\Phi_{\Theta_1}(\mathbf{x}_i)\}_{i=1}^n$, we may solve the its explanatory surrogate function using Eqn.(4).

Corollary 12. *(Representer point selection [7]) The minimizer of Eqn.(4), instantiated with $K_{LL}(\mathbf{x}, \mathbf{z}) = \langle \Phi_{\Theta_1}(\mathbf{x}), \Phi_{\Theta_1}(\mathbf{z}) \rangle, \forall \mathbf{x}, \mathbf{z} \in \mathbb{R}^d$, can be represented as*

$$\hat{f}_K(\cdot) = \sum_{i=1}^n \alpha_i K_{LL}(\mathbf{x}_i, \cdot), \text{ where } \alpha_i = - \frac{1}{n\lambda} \frac{\partial \mathcal{L}(\hat{f}_K(\mathbf{x}_i), f(\mathbf{x}_i))}{\partial \hat{f}_K(\mathbf{x}_i)}, \quad \forall i \in [n]. \quad (12)$$

The above corollary implies that $\hat{\Theta}_2 = \sum_{i=1}^n \alpha_i \Phi_{\Theta_1}(\mathbf{x}_i)$. In other words, the RKHS regularization in Eqn.(4) can be expressed as $\|f_K\|_{\mathcal{H}_K}^2 = \|\Theta_2\|^2$, which is equivalent to L2 regularization. Consequently, the representer point selection method proposed in Yeh et al. [7] can be generalized to our framework when we use last-layer embeddings as feature maps.

5.2 Kernel 2: Neural Tangent Kernels

Although freezing all layers except for the last layer is a straightforward way to simplify neural networks to linear machines, last-layer representers may overlook influential behavior that is present in other layers. For example, Yeh et al. [53] shows that representation in the last layer leads to inferior results for language models. On the other hand, neural

tangent kernels (NTK) [22] have been demonstrated as a more accurate approximation of neural networks [54, 55, 56]. By using NTKs, we use gradients with respect to model parameters as feature maps and approximate neural networks with the corresponding kernel machines. This formulation enables us to derive a generalized representer that captures gradient information of all layers.

For a neural network with scalar output $f_\theta : \mathbb{R}^d \mapsto \mathbb{R}$ parameterized by a vector of parameters $\theta \in \mathbb{R}^p$, the NTK is a kernel $K : \mathbb{R}^d \times \mathbb{R}^d \mapsto \mathbb{R}$ defined by the feature maps $\Phi_\theta(\mathbf{x}) = \frac{\partial f_\theta(\mathbf{x})}{\partial \theta}$:

$$K_{\text{NTK},\theta}(\mathbf{x}, \mathbf{z}) = \left\langle \frac{\partial f_\theta(\mathbf{x})}{\partial \theta}, \frac{\partial f_\theta(\mathbf{z})}{\partial \theta} \right\rangle. \quad (13)$$

Connection to TracIn [6]: TracIn measures *the change in model parameters from the start to the end of training*. While it is intractable due to the need to store model parameters of all iterations, Pruthi et al. [6] used checkpoints(CP) as a practical relaxation: given model parameters $\theta^{(t)}$ and learning rates $\eta^{(t)}$ at all model checkpoints $t = 0, \dots, T$, the formulation of TracInCP is given below³:

$$\begin{aligned} \phi_{\text{TracInCP}}(f_\theta, (\mathbf{x}_i, y_i) \rightarrow \mathbf{x}) &= - \sum_{t=0}^T \eta^{(t)} \frac{\partial \mathcal{L}(f_\theta(\mathbf{x}_i), y_i)}{\partial \theta} \Big|_{\theta=\theta^{(t)}} \frac{\partial f_\theta(\mathbf{x})}{\partial \theta} \Big|_{\theta=\theta^{(t)}} \\ &= - \sum_{t=0}^T \underbrace{\eta^{(t)} \frac{\partial \mathcal{L}(f_\theta(\mathbf{x}_i), y_i)}{\partial f_\theta(\mathbf{x}_i)} \Big|_{\theta=\theta^{(t)}}}_{\text{global importance}} \underbrace{K_{\text{NTK},\theta^{(t)}}(\mathbf{x}_i, \mathbf{x})}_{\text{local importance}}. \end{aligned} \quad (14)$$

When the learning rate is constant throughout the training process, TracInCP can be viewed as a generalized representer instantiated with target derivative as global importances and NTK (Eqn.(13)) as the kernel function, but uses different kernels on different checkpoints.

5.3 Kernel 3: Influence Function Kernel

The influence functions [5] can also be represented as a generalized representer with the following kernel:

$$K_{\text{Inf},\theta}(\mathbf{x}, \mathbf{z}) = \left\langle \frac{\partial f_\theta(\mathbf{x})}{\partial \theta}, \frac{\partial f_\theta(\mathbf{z})}{\partial \theta} \right\rangle_{H_\theta^{-1}} = \frac{\partial f_\theta(\mathbf{x})}{\partial \theta} H_\theta^{-1} \frac{\partial f_\theta(\mathbf{z})}{\partial \theta}, \quad (15)$$

where $H_\theta = \frac{1}{n} \sum_{i=1}^n \frac{\partial^2 \mathcal{L}(f_\theta(\mathbf{x}_i), y_i)}{\partial \theta^2}$ is the Hessian matrix with respect to target model parameters. The influence function then can be written as:

$$\phi_{\text{Inf}}(f_\theta, (\mathbf{x}_i, y_i) \rightarrow \mathbf{x}) = - \frac{\partial \mathcal{L}(f_\theta(\mathbf{x}_i), y_i)}{\partial \theta} H_\theta^{-1} \frac{\partial f_\theta(\mathbf{x})}{\partial \theta} = - \underbrace{\frac{\partial \mathcal{L}(f_\theta(\mathbf{x}_i), y_i)}{\partial f_\theta(\mathbf{x}_i)}}_{\text{global importance}} \underbrace{K_{\text{Inf},\theta}(\mathbf{x}_i, \mathbf{x})}_{\text{local importance}}. \quad (16)$$

Therefore, the influence function can be seen as a member of generalized representers with target derivative global importance (Definition 10) and the influence function kernel. Influence functions [57] were designed to measure *how would the model's predictions change if a training input were perturbed* for convex models trained with empirical risk minimization. Consequently, the inversed Hessian matrix describes the sensitivity of the model parameters in each direction.

6 Experiments

In the experiment, we compare different representers within our proposed framework on both vision and language classification tasks. We use convolutional neural networks (CNN) since they are widely recognized deep neural network architectur. We compare performnce of different choices of kernels and different ways to compute global importance. Existing generalized representers, such as influence functions [5], representer point selections [53], and TracIn [6], are included in our experiment.

³We replace the loss function on the test point $\mathcal{L}(f(\mathbf{x}), y)$ with the target function prediction $f(\mathbf{x})$ to measure training point influence on the predictions.

6.1 Experimental Setups

Evaluation metrics: We use *case deletion diagnostics* [53, 58, 57], $\text{DEL}_-(\mathbf{x}, k, \phi)$, as our primary evaluation metric. The metric measures the difference between models’ prediction score on \mathbf{x} when we remove top- k negative impact samples given by method ϕ and the prediction scores of the original models. We expect DEL_- to be positive since models’ prediction scores should increase when we remove negative impact samples. To evaluate deletion metric at different k , we follow Yeh et al. [53] and report area under the curve (AUC): $\text{AUC-DEL}_- = \sum_{i=1}^m \text{DEL}_-(\mathbf{x}, k_i, \phi)/m$, where $k_1 < k_2 < \dots < k_m$ is a predefined sequence of k .

We choose $k_i = 0.02in$ for $i = 0, 1, \dots, 5$ with n as the size of the training set. The average of each metric is calculated across 50/200 randomly initialized neural networks for vision/language data. For every neural network, sample-based explanation methods are computed for 10 randomly selected testing samples.

Datasets and models being explained: For image classification, we follow Pruthi et al. [6] and use MNIST [59] and CIFAR-10 [60] datasets. For text classification, we follow Yeh et al. [53] and use Toxicity⁴ and AGnews⁵ datasets, which contain toxicity comments and news of different categories respectively. Due to computational challenges in computing deletion diagnostics, we subsample the datasets by transforming them into binary classification problems with each class containing around 6,000 training samples. The CNNs we use for the four datasets comprise 3 layers. For vision datasets, the models contain around 95,000 parameters. For text datasets, the total number of parameters in the model is 1,602,257 with over 90% of the parameters residing in the word embedding layer that contains 30,522 trainable word embeddings of dimensions 48. Please refer to the Appendix C for more details on the implementation of generalized representers and dataset constructions.

Datasets	Methods				
Experiment I - Comparison of different global importance for generalized representers					
Kernels	NTK-final			Random	
Global importance	surrogate derivative	target derivative	tracking	Selection	
MNIST	1.88 ± 0.25	2.41 ± 0.30	3.52 ± 0.48	−0.50 ± 0.16	
CIFAR-10	2.27 ± 0.18	2.81 ± 0.20	3.26 ± 0.19	0.136 ± 0.10	
Toxicity	—	1.10 ± 0.21	2.08 ± 0.23	0.15 ± 0.19	
AGnews	—	1.88 ± 0.27	2.56 ± 0.27	0.19 ± 0.26	
Experiment II - Comparison of different kernels for generalized representers					
Global importance	tracking				
Kernels	last layer-final	NTK-init	NTK-middle	NTK-final	Inf-final
MNIST	3.44 ± 0.46	3.18 ± 0.46	3.63 ± 0.49	3.52 ± 0.48	3.66 ± 0.49
CIFAR-10	2.26 ± 0.13	1.35 ± 0.20	2.67 ± 0.19	3.26 ± 0.19	3.46 ± 0.19
Toxicity	1.34 ± 0.22	0.63 ± 0.22	1.90 ± 0.23	2.08 ± 0.23	0.42 ± 0.20 [†]
AGnews	2.14 ± 0.27	1.81 ± 0.27	2.54 ± 0.28	2.56 ± 0.27	0.92 ± 0.26 [†]
Experiment III - Comparison of different generalized representers					
Methods	Existing generalized representers			Novel generalized representers	
	TracInCP [6]	Influence function [5]	Representer Point [7]	NTK-final (tracking)	Inf-final (tracking)
MNIST	4.20 ± 0.52	2.56 ± 0.32	2.51 ± 0.30	3.52 ± 0.48	3.66 ± 0.49
CIFAR-10	2.84 ± 0.20	3.02 ± 0.21	1.65 ± 0.19	3.26 ± 0.19	3.46 ± 0.19
Toxicity	1.59 ± 0.23	0.26 ± 0.20	0.37 ± 0.19	2.08 ± 0.23	0.42 ± 0.20 [†]
AGnews	2.18 ± 0.27	0.75 ± 0.26	0.86 ± 0.25	2.56 ± 0.27	0.92 ± 0.26 [†]

Table 1: Case deletion diagnostics, AUC-DEL_- , for removing negative impact training samples on four different datasets. 95% confidence interval of averaged deletion diagnostics on $50 \times 10 = 500$ (or $200 \times 10 = 2000$) samples is reported for vision (or language) data. Larger AUC-DEL_- is better. Init, middle, and final denote initial parameters $\theta^{(0)}$, parameters of a middle checkpoint $\theta^{(T/2)}$, and final parameters $\theta^{(T)}$ for neural networks trained with T epochs. [†]We only use the last-layer parameters to compute influence functions as in [5, 53] since the total number of parameters are too large for text models.

⁴<https://www.kaggle.com/c/jigsaw-toxic-comment-classification-challenge>

⁵http://groups.di.unipi.it/gulli/AG_corpus_of_news_articles.html

6.2 Experimental Results

The results are shown in Table 1. We also provide deletion curves we compute AUC-DEL_{...} for in the Appendix.

I. Comparison of different global importance: In the first experiment, we fix the kernel to be the NTK computed on final model parameters, and we compare different methods for computing global importance in Section 4. We do not compute the surrogate derivative on the text datasets since the total numbers of parameters are too large, making the computation infeasible.

We observe that *tracking* has the best performance, followed by *target derivative* and then *surrogate derivative*. This could be due to the loss flattening when converged and the loss gradients becoming less informative. Consequently, accumulating loss gradients during training is the most effective approach. Moreover, if *tracking* is not feasible when training trajectories are not accessible, we may use *target derivative* instead of *surrogate derivative* as an alternative to explain neural networks since they have similar performance.

II. Comparison of different kernels: Next, we fix the global importance to *tracking* and compare different kernels in Section 5. We employ the tracking representers to compute global importance since it showed the best performance in the previous experiment. We can see that the influence function kernel performs the best in the vision data sets, and the NTK-final kernel has the best performance in language data sets. Note that influence functions exhibit distinctly contrasting performances on image and text data, which could be attributed to our reliance solely on last-layer parameters for influence function computation on language datasets. This finding aligns with the conclusions of Yeh et al. [53], who suggest that the last layer gradients provide less informative insights for text classifiers.

In summary, these findings indicate that NTK-final is a dependable kernel selection due to its consistent high performance across all four datasets, while also offering a computational efficiency advantage over the influence function kernel. These results also demonstrate that accessing target model checkpoints for computing kernels is unnecessary since NTK and influence function on the final model already provide informative feature maps.

III. Comparison of different generalized representers: Finally, we compare the new generalized representer with other existing generalized representers. We categorize TracInCP, the influence function, and the representer point as existing generalized representers: TracInCP can be viewed as an ensemble of generalized representers with target derivatives using the Neural Tangent Kernel. The influence function can be expressed as the influence function kernel with the target derivative. Lastly, the representer point can be seen as a form of generalized representer that utilizes the last-layer kernel and the surrogate derivative.

We find that the Inf-final has comparable performance to TracInCP and they outperform other approaches. Although TracInCP has the best performance on MNIST, it requires accessing different checkpoints, which requires a significant amount of memory and time complexity. In contrast, the NTK and Inf tracking representers are more efficient since they only require tracking gradient descent trajectories during training without the need for storing checkpoints.

7 Conclusion and Future work

In this work, we present *generalized representers* that are the only class of sample based explanations that satisfy a set of desirable axiomatic properties. We explore various techniques for computing generalized representers in the context of modern non-linear machine learning models and show that many popular existing methods fall into this category. Additionally, we propose tracking representers that track sample importance along the gradient descent trajectory. In future work, it would be of interest to derive different generalized representers by altering different global importance and choices of kernels, as well as investigating their applicability to diverse machine learning models and modalities.

8 Acknowledgements

We acknowledge the support of DARPA via FA8750-23-2-1015, ONR via N00014-23-1-2368, and NSF via IIS-1909816.

References

- [1] Marco Tulio Ribeiro, Sameer Singh, and Carlos Guestrin. Why should i trust you?: Explaining the predictions of any classifier. In *Proceedings of the 22nd ACM SIGKDD international conference on knowledge discovery and data mining*, pages 1135–1144. ACM, 2016.
- [2] Ramprasaath R Selvaraju, Michael Cogswell, Abhishek Das, Ramakrishna Vedantamand, Devi Parikh, and Dhruv Parikh. Grad-cam: Visual explanations from deep networks via gradient-based localization. *International conference on computer vision*, 2017.
- [3] Daniel Smilkov, Nikhil Thorat, Been Kim, Fernanda Viégas, and Martin Wattenberg. Smoothgrad: removing noise by adding noise. *arXiv preprint arXiv:1706.03825*, 2017.

- [4] Scott M Lundberg and Su-In Lee. A unified approach to interpreting model predictions. In *Advances in Neural Information Processing Systems*, pages 4765–4774, 2017.
- [5] Pang Wei Koh and Percy Liang. Understanding black-box predictions via influence functions. In *Proceedings of the 34th International Conference on Machine Learning-Volume 70*, pages 1885–1894. JMLR. org, 2017.
- [6] Garima Pruthi, Frederick Liu, Satyen Kale, and Mukund Sundararajan. Estimating training data influence by tracing gradient descent. *Advances in Neural Information Processing Systems*, 33, 2020.
- [7] Chih-Kuan Yeh, Joon Kim, Ian En-Hsu Yen, and Pradeep K Ravikumar. Representer point selection for explaining deep neural networks. In *Advances in Neural Information Processing Systems*, pages 9291–9301, 2018.
- [8] Amirata Ghorbani and James Zou. Data shapley: Equitable valuation of data for machine learning. In *International Conference on Machine Learning*, pages 2242–2251. PMLR, 2019.
- [9] Satyapriya Krishna, Tessa Han, Alex Gu, Javin Pombra, Shahin Jabbari, Steven Wu, and Himabindu Lakkaraju. The disagreement problem in explainable machine learning: A practitioner’s perspective. *arXiv preprint arXiv:2202.01602*, 2022.
- [10] W James Murdoch, Chandan Singh, Karl Kumbier, Reza Abbasi-Asl, and Bin Yu. Definitions, methods, and applications in interpretable machine learning. *Proceedings of the National Academy of Sciences*, 116(44): 22071–22080, 2019.
- [11] Finale Doshi-Velez and Been Kim. Towards a rigorous science of interpretable machine learning. *arXiv preprint arXiv:1702.08608*, 2017.
- [12] Blair Bilodeau, Natasha Jaques, Pang Wei Koh, and Been Kim. Impossibility theorems for feature attribution. *arXiv preprint arXiv:2212.11870*, 2022.
- [13] Valerie Chen, Nari Johnson, Nicholay Topin, Gregory Plumb, and Ameet Talwalkar. Use-case-grounded simulations for explanation evaluation. *arXiv preprint arXiv:2206.02256*, 2022.
- [14] Kasun Amarasinghe, Kit T Rodolfa, Sérgio Jesus, Valerie Chen, Vladimir Balayan, Pedro Saleiro, Pedro Bizarro, Ameet Talwalkar, and Rayid Ghani. On the importance of application-grounded experimental design for evaluating explainable ml methods. *arXiv preprint arXiv:2206.13503*, 2022.
- [15] Lloyd S Shapley. A value for n-person games. *Contributions to the Theory of Games*, 2(28):307–317, 1953.
- [16] Mukund Sundararajan, Ankur Taly, and Qiqi Yan. Axiomatic attribution for deep networks. In *International Conference on Machine Learning*, 2017.
- [17] Chih-Kuan Yeh, Cheng-Yu Hsieh, Arun Suggala, David I Inouye, and Pradeep K Ravikumar. On the (in) fidelity and sensitivity of explanations. *Advances in Neural Information Processing Systems*, 32, 2019.
- [18] Che-Ping Tsai, Chih-Kuan Yeh, and Pradeep Ravikumar. Faith-shap: The faithful shapley interaction index. *Journal of Machine Learning Research*, 24(94):1–42, 2023.
- [19] Mukund Sundararajan, Kedar Dhamdhere, and Ashish Agarwal. The shapley taylor interaction index. In *International Conference on Machine Learning*, pages 9259–9268. PMLR, 2020.
- [20] Chih-Kuan Yeh, Been Kim, Sercan Arik, Chun-Liang Li, Tomas Pfister, and Pradeep Ravikumar. On completeness-aware concept-based explanations in deep neural networks. *Advances in Neural Information Processing Systems*, 33:20554–20565, 2020.
- [21] Bernhard Schölkopf, Ralf Herbrich, and Alex J Smola. A generalized representer theorem. In *International conference on computational learning theory*, pages 416–426. Springer, 2001.
- [22] Arthur Jacot, Franck Gabriel, and Clément Hongler. Neural tangent kernel: Convergence and generalization in neural networks. *Advances in neural information processing systems*, 31, 2018.
- [23] Scott M Lundberg, Gabriel G Erion, and Su-In Lee. Consistent individualized feature attribution for tree ensembles. *arXiv preprint arXiv:1802.03888*, 2018.
- [24] Zayd Hammoudeh and Daniel Lowd. Training data influence analysis and estimation: A survey. *arXiv preprint arXiv:2212.04612*, 2022.
- [25] Tianhao Wang and Ruoxi Jia. Data banzhaf: A data valuation framework with maximal robustness to learning stochasticity. *arXiv preprint arXiv:2205.15466*, 2022.
- [26] Andrew Ilyas, Sung Min Park, Logan Engstrom, Guillaume Leclerc, and Aleksander Madry. Datamodels: Predicting predictions from training data. *arXiv preprint arXiv:2202.00622*, 2022.
- [27] Yongchan Kwon and James Zou. Beta shapley: a unified and noise-reduced data valuation framework for machine learning. *arXiv preprint arXiv:2110.14049*, 2021.

- [28] Tom Yan and Ariel D Procaccia. If you like shapley then you’ll love the core. In *Proceedings of the AAAI Conference on Artificial Intelligence*, volume 35, pages 5751–5759, 2021.
- [29] Chiyuan Zhang, Daphne Ippolito, Katherine Lee, Matthew Jagielski, Florian Tramèr, and Nicholas Carlini. Counterfactual memorization in neural language models. *arXiv preprint arXiv:2112.12938*, 2021.
- [30] Ziheng Jiang, Chiyuan Zhang, Kunal Talwar, and Michael C Mozer. Characterizing structural regularities of labeled data in overparameterized models. *arXiv preprint arXiv:2002.03206*, 2020.
- [31] Ruoxi Jia, Fan Wu, Xuehui Sun, Jiachen Xu, David Dao, Bhavya Kailkhura, Ce Zhang, Bo Li, and Dawn Song. Scalability vs. utility: Do we have to sacrifice one for the other in data importance quantification? In *Proceedings of the IEEE/CVF Conference on Computer Vision and Pattern Recognition*, pages 8239–8247, 2021.
- [32] Jinsung Yoon, Sercan Arik, and Tomas Pfister. Data valuation using reinforcement learning. In *International Conference on Machine Learning*, pages 10842–10851. PMLR, 2020.
- [33] Amirata Ghorbani, Michael Kim, and James Zou. A distributional framework for data valuation. In *International Conference on Machine Learning*, pages 3535–3544. PMLR, 2020.
- [34] Ruoxi Jia, David Dao, Boxin Wang, Frances Ann Hubis, Nick Hynes, Nezihe Merve Gürel, Bo Li, Ce Zhang, Dawn Song, and Costas J Spanos. Towards efficient data valuation based on the shapley value. In *The 22nd International Conference on Artificial Intelligence and Statistics*, pages 1167–1176. PMLR, 2019.
- [35] Yuanyuan Chen, Boyang Li, Han Yu, Pengcheng Wu, and Chunyan Miao. Hydra: Hypergradient data relevance analysis for interpreting deep neural networks. In *Proceedings of the AAAI Conference on Artificial Intelligence*, volume 35, pages 7081–7089, 2021.
- [36] Yi Sui, Ga Wu, and Scott Sanner. Representer point selection via local jacobian expansion for post-hoc classifier explanation of deep neural networks and ensemble models. *Advances in neural information processing systems*, 34:23347–23358, 2021.
- [37] Jonathan Brophy, Zayd Hammoudeh, and Daniel Lowd. Adapting and evaluating influence-estimation methods for gradient-boosted decision trees. *arXiv preprint arXiv:2205.00359*, 2022.
- [38] Sung Min Park, Kristian Georgiev, Andrew Ilyas, Guillaume Leclerc, and Aleksander Madry. Trak: Attributing model behavior at scale. *arXiv preprint arXiv:2303.14186*, 2023.
- [39] Andrew Silva, Rohit Chopra, and Matthew Gombolay. Cross-loss influence functions to explain deep network representations. In *International Conference on Artificial Intelligence and Statistics*, pages 1–17. PMLR, 2022.
- [40] Andrea Schioppa, Polina Zablotskaia, David Vilar, and Artem Sokolov. Scaling up influence functions. In *Proceedings of the AAAI Conference on Artificial Intelligence*, volume 36, pages 8179–8186, 2022.
- [41] Rui Zhang and Shihua Zhang. Rethinking influence functions of neural networks in the over-parameterized regime. In *Proceedings of the AAAI Conference on Artificial Intelligence*, volume 36, pages 9082–9090, 2022.
- [42] Samyadeep Basu, Philip Pope, and Soheil Feizi. Influence functions in deep learning are fragile. *arXiv preprint arXiv:2006.14651*, 2020.
- [43] Han Guo, Nazneen Fatema Rajani, Peter Hase, Mohit Bansal, and Caiming Xiong. Fastif: Scalable influence functions for efficient model interpretation and debugging. *arXiv preprint arXiv:2012.15781*, 2020.
- [44] Elnaz Barshan, Marc-Etienne Brunet, and Gintare Karolina Dziugaite. Relatif: Identifying explanatory training samples via relative influence. In *International Conference on Artificial Intelligence and Statistics*, pages 1899–1909. PMLR, 2020.
- [45] Samyadeep Basu, Xuchen You, and Soheil Feizi. On second-order group influence functions for black-box predictions. In *International Conference on Machine Learning*, pages 715–724. PMLR, 2020.
- [46] Hugo Thimonier, Fabrice Popineau, Arpad Rimmel, Bich-Liên Doan, and Fabrice Daniel. Tracinad: Measuring influence for anomaly detection. In *2022 International Joint Conference on Neural Networks (IJCNN)*, pages 1–6. IEEE, 2022.
- [47] Satoshi Hara, Atsushi Nitanda, and Takanori Maehara. Data cleansing for models trained with sgd. *Advances in Neural Information Processing Systems*, 32, 2019.
- [48] Maximilian Mozes, Tolga Bolukbasi, Ann Yuan, Frederick Liu, Nithum Thain, and Lucas Dixon. Gradient-based automated iterative recovery for parameter-efficient tuning. *arXiv preprint arXiv:2302.06598*, 2023.
- [49] Lloyd S. Shapley. *A value for n-person games*, page 31–40. Cambridge University Press, 1988. doi: 10.1017/CBO9780511528446.003.
- [50] Arun Suggala, Adarsh Prasad, and Pradeep K Ravikumar. Connecting optimization and regularization paths. *Advances in Neural Information Processing Systems*, 31, 2018.

- [51] Jaehoon Lee, Yasaman Bahri, Roman Novak, Samuel S Schoenholz, Jeffrey Pennington, and Jascha Sohl-Dickstein. Deep neural networks as gaussian processes. *arXiv preprint arXiv:1711.00165*, 2017.
- [52] Richard Zhang, Phillip Isola, Alexei A Efros, Eli Shechtman, and Oliver Wang. The unreasonable effectiveness of deep features as a perceptual metric. In *Proceedings of the IEEE conference on computer vision and pattern recognition*, pages 586–595, 2018.
- [53] Chih-Kuan Yeh, Ankur Taly, Mukund Sundararajan, Frederick Liu, and Pradeep Ravikumar. First is better than last for training data influence. *arXiv preprint arXiv:2202.11844*, 2022.
- [54] Alexander Wei, Wei Hu, and Jacob Steinhardt. More than a toy: Random matrix models predict how real-world neural representations generalize. In *International Conference on Machine Learning*, pages 23549–23588. PMLR, 2022.
- [55] Philip M Long. Properties of the after kernel. *arXiv preprint arXiv:2105.10585*, 2021.
- [56] Sadhika Malladi, Alexander Wettig, Dingli Yu, Danqi Chen, and Sanjeev Arora. A kernel-based view of language model fine-tuning. *arXiv preprint arXiv:2210.05643*, 2022.
- [57] R Dennis Cook and Sanford Weisberg. *Residuals and influence in regression*. New York: Chapman and Hall, 1982.
- [58] Xiaochuang Han, Byron C Wallace, and Yulia Tsvetkov. Explaining black box predictions and unveiling data artifacts through influence functions. *arXiv preprint arXiv:2005.06676*, 2020.
- [59] Yann LeCun and Corinna Cortes. MNIST handwritten digit database. 2010. URL <http://yann.lecun.com/exdb/mnist/>.
- [60] Alex Krizhevsky, Geoffrey Hinton, et al. Learning multiple layers of features from tiny images. 2009.
- [61] Diederik P Kingma and Jimmy Ba. Adam: A method for stochastic optimization. *arXiv preprint arXiv:1412.6980*, 2014.
- [62] Naman Agarwal, Brian Bullins, and Elad Hazan. Second-order stochastic optimization in linear time. *stat*, 1050: 15, 2016.
- [63] James Mercer. Xvi. functions of positive and negative type, and their connection the theory of integral equations. *Philosophical transactions of the royal society of London. Series A, containing papers of a mathematical or physical character*, 209(441-458):415–446, 1909.

A Overview

The appendix is organized as follows: First, in Section B, we discuss the potential social impacts of our work. Next, in Section C, we provide experimental details on the qualitative measurements on image classification datasets presented in Section 6. Then, in Section D, we illustrate the extension of generalized representers to explain vector-output target functions. Finally, we provide proofs of our theoretical results in Section E.

B Potential Negative Social Impact of Our Work

Our approach has the potential to bring about various social consequences by allowing individuals to modify model predictions through adjustments to training samples. These effects can involve the risks of attacking established models or exacerbating biases and ethical concerns.

C More Experimental Details

C.1 More details on datasets and models being explained

Specifically, for MNIST, we perform classification on digits 1 and 5, with each class consisting of around 6,000 images. For CIFAR-10, we conduct classification between the airplane and automobile classes, each class containing 5,000 images. For the toxicity dataset, we select a subset of 6,000 sentences each for both toxic and non-toxic labels. Regarding the AGnews dataset, we focus exclusively on the world and sports categories with each class containing 6,000 text sequences.

The CNNs we use for vision datasets comprise 3 layers and approximately 95,000 parameters. They are trained with SGD optimizer with learning rates 0.3/0.2 with $T = 30/60$ epochs for MNIST/CIFAR-10 respectively. Their averaged test accuracies over 50 trials are 97.93%/92.40% on test sets of size 2,000 for MNIST/CIFAR-10.

For text datasets, We employ three-layer convolutional neural networks. The model architecture is as follows: input texts are initially transformed into token embeddings with a dimension of 48 and a vocabulary size of 30,522. This is followed by three convolutional layers, each consisting of 50 kernels of size 5. A global max pooling layer and a fully connected layer are then applied. The total number of parameters in the model is 1,602,257, with more than 90% of the parameters residing in the word embedding layer. The models are trained with Adam optimizer [61] with default learning rates 0.001 using $T = 10$ epochs. They have average 80.44%/92.78% test accuracy on Toxicity/Agnews datasets respectively.

Due to the large number of parameters in the target model (over 1.6 million), we do not implement the generalized representer with surrogate derivative global importance and neural tangent kernel since it is impractical to store all feature maps of training samples. Also, we apply the influence function only on the last layer [6] since the computation of the inverse Hessian matrix is too costly.

C.2 Computation of Global Importances

We use the three methods mentioned in Section 4, which are *surrogate derivative*, *target derivative*, and *tracking representers*.

Surrogate derivative: We first transform Eqn.(4) to the primal form: let $f_K(\mathbf{x}) = \langle \theta_{\text{sug}}, \Phi(\mathbf{x}) \rangle$ be a kernel machine that has finite-dimensional feature maps and is parameterized by θ_{sug} . Eqn.(4) can then be transformed to:

$$\theta_{\text{sug}}^* = \underset{\theta_{\text{sug}} \in \mathbb{R}^p}{\operatorname{argmin}} \frac{1}{n} \sum_{i=1}^n \mathcal{L}(\langle \theta_{\text{sug}}, \Phi(\mathbf{x}_i) \rangle, f(\mathbf{x}_i)) + \frac{\lambda}{2} \|\theta_{\text{sug}}\|^2. \quad (17)$$

We then follow Yeh et al. [7] to take the target model parameters as initialization and use the line-search gradient descent algorithm to solve Eqn.(17). When the kernel function is chosen as a neural tangent kernel, we have an extra bias term: $f_K(\mathbf{x}) = \sum_{i=1}^n \langle \partial_{\theta} f_{\theta}(\mathbf{x}_i), \theta_{\text{sug}} - \theta \rangle + f_{\theta}(\mathbf{x})$, where θ is the parameters of the target function f_{θ} . The optimization problem then becomes

$$\theta_{\text{sug}}^* = \underset{\theta_{\text{sug}} \in \mathbb{R}^p}{\operatorname{argmin}} \frac{1}{n} \sum_{i=1}^n \mathcal{L}(\langle \theta_{\text{sug}} - \theta, \partial_{\theta} f_{\theta}(\mathbf{x}_i) \rangle + f_{\theta}(\mathbf{x}_i), f_{\theta}(\mathbf{x}_i)) + \frac{\lambda}{2} \|\theta_{\text{sug}}\|^2. \quad (18)$$

We set the regularization parameter $\lambda = 2 \times 10^{-2}$ in our experiments. Then we compute the global importance with Eqn.(6), i.e.

$$\alpha_i = \frac{\partial \mathcal{L}(\langle \theta_{\text{sug}}^* - \theta, \partial_{\theta} f_{\theta}(\mathbf{x}_i) \rangle + f_{\theta}(\mathbf{x}_i), f_{\theta}(\mathbf{x}_i))}{\partial \langle \theta_{\text{sug}} - \theta, \partial_{\theta} f_{\theta}(\mathbf{x}_i) \rangle}.$$

Target derivative: We directly adopt Eqn.(7) that computes derivatives of the loss function with respect to the target function predictions.

Tracking representers: In our experiment, we use the following relaxation for further speed up:

$$\alpha_i^* = - \sum_{t \in [T]: i \in B^{(t)}} \frac{\eta^{(t)}}{|B^{(t)}|} \frac{\partial \mathcal{L}(f^{(t-1)}(\mathbf{x}_i), y_i)}{\partial f^{(t-1)}(\mathbf{x}_i)}, \quad (19)$$

where we assume the target model is trained with (stochastic) gradient descent, $f^{(t)}(\mathbf{x}_i)$ denotes the target model at t^{th} iteration during training, and $B^{(t)}$ and $\eta^{(t)}$ are the corresponding mini-batch and learning rate. Similar to the intuition of replacing the surrogate derivative with target derivative, we track the target model's training trajectory directly instead of solving Eqn.(4) with kernel gradient descent.

C.3 Computation of Kernel functions

For last layer embeddings and neural tangent kernels, we directly use Eqn.(11) and Eqn.(15) to compute feature maps. For influence function kernels, we use public implementation for Pytorch⁶. It uses stochastic estimation [62] to speed up the computation of the inversed hessian vector product and sets the damping factor to 0.01.

C.4 Computation of TracInCP [6]

For TracInCP, we compute over 7 evenly spaced checkpoints, including the initial parameter $\theta^{(0)}$ and the final parameter $\theta^{(T)}$.

C.5 Hardware usage

For all of our experiments, we use 4 NVIDIA A6000 GPUs each with 40GB of memory and 96 CPU cores. To run the experiment on the vision datasets in Section 6, we retrain the model over

$$11 \text{ (number of methods)} \times 2 \text{ (for AUC-DEL}_+ \text{ and AUC-DEL}_- \text{)} \times 50 \text{ (number of random seeds)} \times 10 \text{ (number of test samples per model)} = 11,000 \text{ times .}$$

We train 5 models simultaneously on a single GPU for speed up. It takes around 4 days to run the experiment in Section 6.

C.6 Supplementary Experimental Results

Apart from the numerical results in terms of AUC-DEL₋, we also provide deletion curves showing changes in model predictions for different numbers of training samples being removed in Figure 1, 2, 3 and 4.

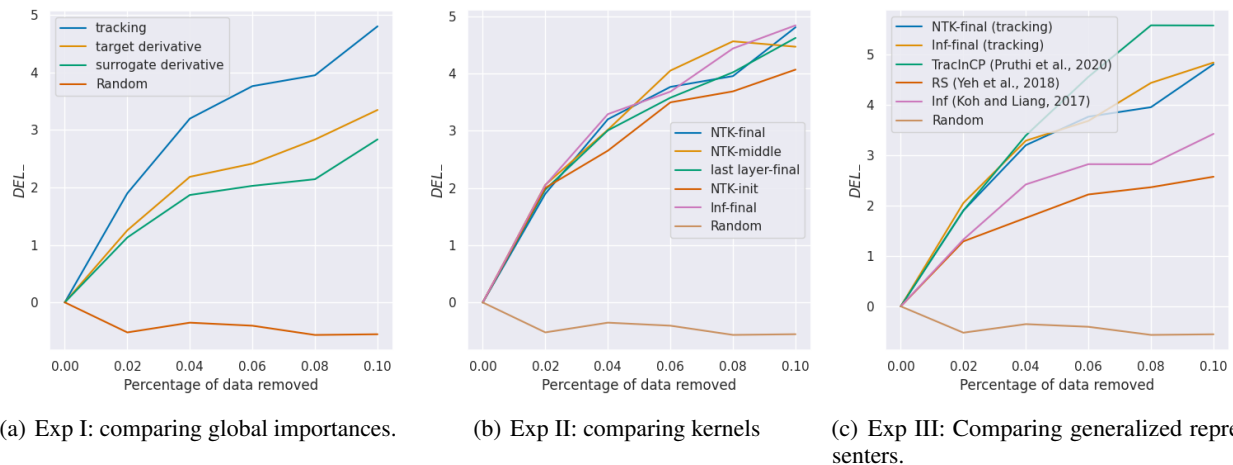
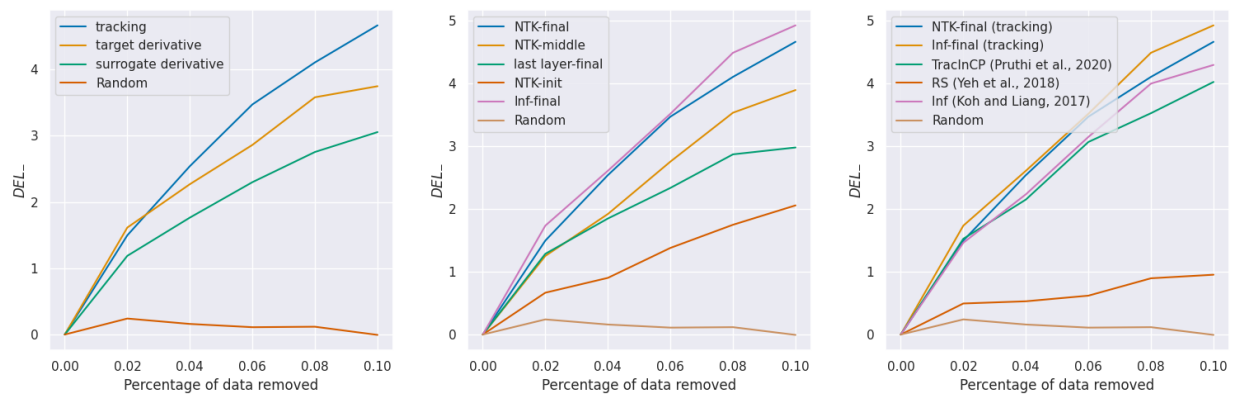


Figure 1: Deletion curves for the **MNIST dataset**. Larger DEL_- is better since it indicates a method finds more negative impact training samples.

C.7 Licence of Datasets

For the image classification datasets, MNIST [59] has GNU general public license v3.0. The CIFAR-10 dataset is under MIT License. The Toxicity dataset has license cc0-1.0 The AGnews dataset has licensed non-commercial use.

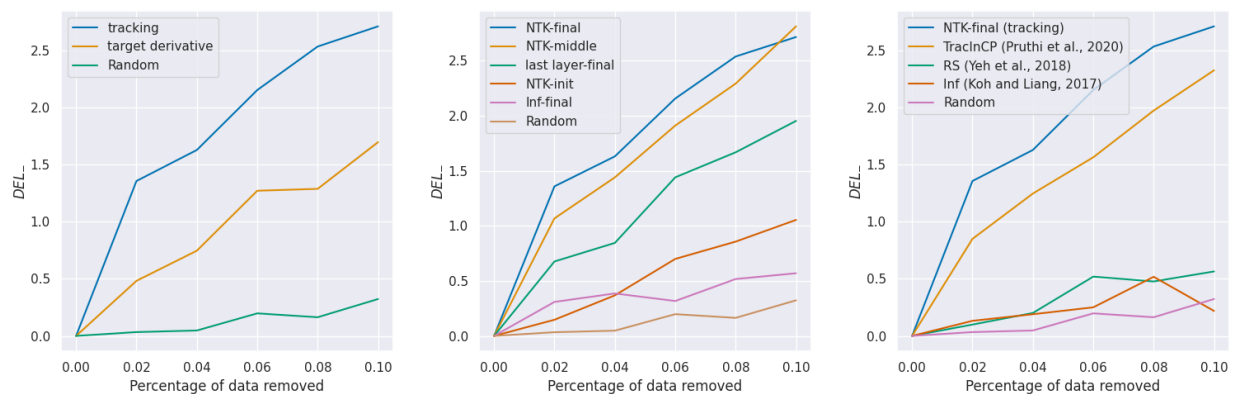
⁶https://github.com/nimarb/pytorch_influence_functions



(a) Exp I: comparing global importances.

(b) Exp II: comparing kernels

(c) Exp III: Comparing generalized representers.

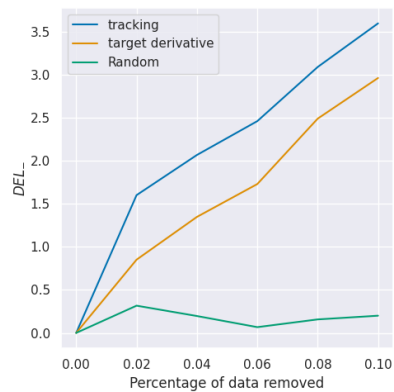
Figure 2: Deletion curves for the **CIFAR-10 dataset**. Larger DEL_- is better since it indicates a method finds more negative impact training samples.

(a) Exp I: comparing global importances.

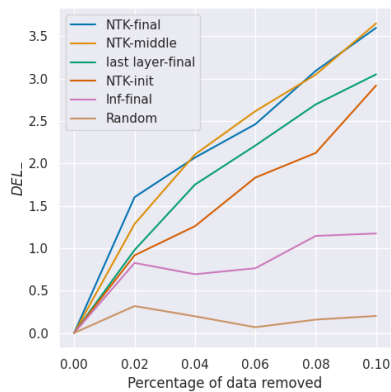
(b) Exp II: comparing kernels

(c) Exp III: Comparing generalized representers.

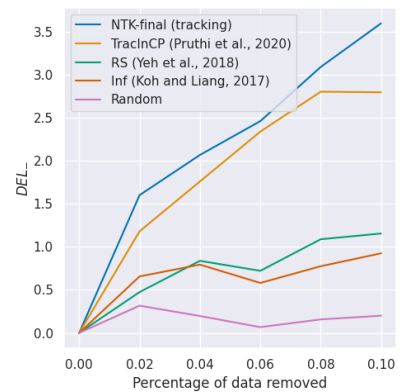
Figure 3: Deletion curves for the **Toxicity dataset**. Larger DEL_- is better since it indicates a method finds more negative impact training samples.



(a) Exp I: comparing global importances.



(b) Exp II: comparing kernels



(c) Exp III: Comparing generalized representers.

Figure 4: Deletion curves for the **AGnews dataset**. Larger DEL_- is better since it indicates a method finds more negative impact training samples.

D Extension to Explain Vector Output Target Functions

In the main paper, we assume that the target function has a scalar output for notational convenience. However, most modern machine models have multi-dimensional outputs as is common for multi-class classification problems. In this section, we show that generalized representers can be extended to vector output by utilizing kernels for vector-valued functions.

Definitions: Given a target function $f : \mathbb{R}^d \mapsto \mathbb{R}^c$, a dataset $\mathcal{D} := \{(\mathbf{x}_i, y_i)\}_{i=1}^n$ with each training sample $(\mathbf{x}_i, y_i) \in \mathbb{R}^d \times \mathcal{Y}$, and a Mercer kernel $K : \mathbb{R}^d \times \mathbb{R}^d \mapsto \mathbb{R}^{c \times c}$, the generalized representer has the following form:

$$\phi(f, (\mathbf{x}_i, y_i) \rightarrow \mathbf{x}) = \boldsymbol{\alpha}_i^\top K(\mathbf{x}_i, \mathbf{x}) \in \mathbb{R}^c, \quad \forall i \in [n], \quad (20)$$

where the global importance $\boldsymbol{\alpha} \in \mathbb{R}^{n \times c}$ is a matrix with α_{ij} the importance of the i^{th} training sample to the j^{th} prediction, and $\boldsymbol{\alpha}_i \in \mathbb{R}^{c \times 1}$ is the i^{th} row of the matrix.

D.1 Vector-valued Global Importance

We discuss the extension of the three methods in Section 4, which are *surrogate derivative*, *target derivative*, and *tracking representers*, for vector-valued target functions.

Surrogate derivative: The surrogate derivative in Eqn.(6) for vector-valued target functions is:

$$\boldsymbol{\alpha}_{ij}^{\text{sur}} = -\frac{1}{n\lambda} \frac{\partial \mathcal{L}(\hat{f}_K(\mathbf{x}_i), f(\mathbf{x}_i))}{\partial \hat{f}_K(\mathbf{x}_i)_j}, \quad \forall i \in [n] \text{ and } \forall j \in [c], \quad (21)$$

where $\hat{f}_K : \mathbb{R}^p \mapsto \mathbb{R}^c$ is the minimizer of Eqn.(4), and $\hat{f}_K(\mathbf{x}_i)_j$ is its j^{th} output. Eqn.(6) can be obtained by taking derivative of Eqn.(4) with respect to $\boldsymbol{\alpha}_{ij}$.

Target derivative: The target derivative can be represented as

$$\boldsymbol{\alpha}_{ij}^{\text{tar}} = -\frac{1}{n\lambda} \frac{\partial \mathcal{L}(f(\mathbf{x}_i), y_i)}{\partial f(\mathbf{x}_i)_j}, \quad \forall i \in [n] \text{ and } \forall j \in [c], \quad (22)$$

where $f(\mathbf{x}_i)_j$ denotes j^{th} output of the target function evaluated on \mathbf{x}_i .

Tracking representers: The formulation of the tracking representers for vector-valued target functions is as below:

$$\boldsymbol{\alpha}_{ij}^{\text{tra}} = -\sum_{t \in [T] : i \in B^{(t)}} \frac{\eta^{(t)}}{|B^{(t)}|} \frac{\partial \mathcal{L}(f_K^{(t-1)}(\mathbf{x}_i), f(\mathbf{x}_i))}{\partial f_K^{(t-1)}(\mathbf{x}_i)_j} \quad \forall i \in [n] \text{ and } \forall j \in [c], \quad (23)$$

where $B^{(t)}$ and $\eta^{(t)}$ denote the minibatch and the learning rate used to solve Eqn.(4), and $\hat{f}_K^{(t-1)}$ is the function at the $(t-1)^{\text{th}}$ time step and $\hat{f}_K^{(t-1)}(\mathbf{x}_i)_j$ denotes its j^{th} output of $\hat{f}_K^{(t-1)}(\mathbf{x}_i)$.

D.2 Kernels for Vector-valued Target Functions

In this section, we provide formulas for kernels mentioned in Section 5 for vector-valued target functions.

Penultimate-layer embeddings: Let the target model f be $f(\mathbf{x}) = \Phi_{\Theta_1}(\mathbf{x})^\top \Theta_2$, where $\Phi_{\Theta_1} : \mathbb{R}^d \mapsto \mathbb{R}^\ell$ maps inputs to the penultimate layer, and $\Theta_2 \in \mathbb{R}^{\ell \times c}$ is the last layer weight matrix. The kernel function is defined as

$$K_{\text{LL}}(\mathbf{x}, \mathbf{z}) = \langle \Phi_{\Theta_1}(\mathbf{x}), \Phi_{\Theta_1}(\mathbf{z}) \rangle \cdot \mathbb{I}_c \in \mathbb{R}^{c \times c}, \quad \forall \mathbf{x}, \mathbf{z} \in \mathbb{R}^d, \quad (24)$$

where \mathbb{I}_c is the $c \times c$ identity matrix. Since the kernel outputs the same value for all entries on the diagonal, we can consider the target function $f(\mathbf{x}) = [f_1(\mathbf{x}), \dots, f_c(\mathbf{x})]$ as c distinct scalar output functions and compute generalized representers for each of these functions.

Neural tangent kernel: When the target function has multi-dimensional outputs, the neural tangent kernel, $K : \mathbb{R}^d \times \mathbb{R}^d \mapsto \mathbb{R}^{c \times c}$, is defined by

$$K_{\text{NTK}, \theta}(\mathbf{x}, \mathbf{z}) = \left(\frac{\partial f_\theta(\mathbf{x})}{\partial \theta} \right) \left(\frac{\partial f_\theta(\mathbf{z})}{\partial \theta} \right)^\top, \quad (25)$$

where $\frac{\partial f_\theta}{\partial \theta} \in \mathbb{R}^{c \times p}$ is the Jacobian matrix consisting of derivative of the function f_θ with respect to its parameter θ .

Influence function kernel: let $\frac{\partial f_\theta}{\partial \theta} \in \mathbb{R}^{c \times p}$ is the Jacobian matrix defined above, the influence function kernel can be defined as

$$K_{\text{Inf},\theta}(\mathbf{x}, \mathbf{z}) = \frac{\partial f_\theta(\mathbf{x})^\top}{\partial \theta} H_\theta^{-1} \frac{\partial f_\theta(\mathbf{z})}{\partial \theta}. \quad (26)$$

The influence function then can be written as

$$\phi_{\text{Inf}}(f_\theta, (\mathbf{x}_i, y_i) \rightarrow \mathbf{x}) = -\frac{\partial \mathcal{L}(f_\theta(\mathbf{x}_i), y_i)}{\partial \theta} H_\theta^{-1} \frac{\partial f_\theta(\mathbf{x})}{\partial \theta} \quad (27)$$

$$= -\underbrace{\left(\frac{\partial \mathcal{L}(f_\theta(\mathbf{x}_i), y_i)}{\partial f_\theta(\mathbf{x}_i)} \right)^\top}_{\text{global importance}} \underbrace{K_{\text{Inf},\theta}(\mathbf{x}_i, \mathbf{x})}_{\text{local importance}}. \quad (28)$$

E Proof of Theoretical Results

In this section, we prove our theoretical results.

E.1 Proof of Theorem 7

Proof. We first prove that if explanation $\phi(\cdot)$ satisfies the continuity, self-explanation, symmetric zero, symmetric cycle, and irreducibility axioms for any training samples \mathcal{D} containing n training samples $(\mathbf{x}_i, y_i) \in \mathbb{R}^d \times \mathbb{R}$ for all $i \in [n]$, we have

$$\phi(f, \mathbf{x}_i \rightarrow \mathbf{x}_j) = \alpha_i K(\mathbf{x}_i, \mathbf{x}_j), \forall i, j \in [n],$$

for some $\alpha \in \mathbb{R}^n$ and some continuous positive-definite kernel $K : \mathbb{R}^d \times \mathbb{R}^d \mapsto \mathbb{R}$.

Definitions: We first split the training data $\{(\mathbf{x}_i, y_i)\}_{i=1}^n$ into two parts: (1) $\{\mathbf{x}_i\}_{i=1}^m$ such that $\phi(f, \mathbf{x}_i \rightarrow \mathbf{x}_i) \neq 0$, and (2) $\{\mathbf{x}_i, y_i\}_{i=m+1}^n$ such that $\phi(f, \mathbf{x}_i \rightarrow \mathbf{x}_i) = 0$.

We then construct an undirected graph where the points are all training data points $\{\mathbf{x}_i\}_{i=1}^m$ such that $\phi(f, \mathbf{x}_i \rightarrow \mathbf{x}_i) \neq 0$. An edge exists between \mathbf{x}_i and \mathbf{x}_j if $\phi(f, \mathbf{x}_i \rightarrow \mathbf{x}_j) \neq 0$ and $\phi(f, \mathbf{x}_j \rightarrow \mathbf{x}_i) \neq 0$. Now, assume that the graph exists t connected components, and we choose a training point as the reference point in each connected component. Thus, if $\mathbf{x}_i, \mathbf{x}_j$ are connected in the graph, they have the same reference point.

For a training point \mathbf{x}_i , we can assume that the reference point in the connected component that \mathbf{x}_i belongs in is \mathbf{x}_r , we can find a path p from \mathbf{x}_i to \mathbf{x}_r so that $p_0 = i, p_k = r$, and $\phi(f, \mathbf{x}_{p_j} \rightarrow \mathbf{x}_{p_{j+1}}) \neq 0$ for all $j \in [0, k-1]$. Define

$$\alpha'_i = \begin{cases} 1 & , \text{ if } \mathbf{x}_i \text{ is the reference point.} \\ \frac{\phi(f, \mathbf{x}_{p_1} \rightarrow \mathbf{x}_i)}{\phi(f, \mathbf{x}_i \rightarrow \mathbf{x}_{p_1})} \cdots \frac{\phi(f, \mathbf{x}_r \rightarrow \mathbf{x}_{p_{k-1}})}{\phi(f, \mathbf{x}_{p_{k-1}} \rightarrow \mathbf{x}_r)} & , \text{ if } \mathbf{x}_i \text{ is in a connected component with reference point } \mathbf{x}_r. \\ 0 & , \text{ if } i \in \{m+1, \dots, n\} \end{cases}$$

By symmetric cycle axiom, α'_i is well defined and independent of how p is chosen since if two distinct paths connect \mathbf{x}_i to \mathbf{x}_r , α'_i by calculating through both paths will be equal by the symmetric cycle axiom. Formally, define $\alpha'_i(p) = \frac{\phi(f, \mathbf{x}_{p_1} \rightarrow \mathbf{x}_i)}{\phi(f, \mathbf{x}_i \rightarrow \mathbf{x}_{p_1})} \cdots \frac{\phi(f, \mathbf{x}_r \rightarrow \mathbf{x}_{p_{k-1}})}{\phi(f, \mathbf{x}_{p_{k-1}} \rightarrow \mathbf{x}_r)}$, we have

$$\frac{\alpha'_i(p)}{\alpha'_i(q)} = \frac{\phi(f, \mathbf{x}_{p_1} \rightarrow \mathbf{x}_{p_0})}{\phi(f, \mathbf{x}_{p_0} \rightarrow \mathbf{x}_{p_1})} \cdots \frac{\phi(f, \mathbf{x}_{p_k} \rightarrow \mathbf{x}_{p_{k-1}})}{\phi(f, \mathbf{x}_{p_{k-1}} \rightarrow \mathbf{x}_{p_k})} \cdot \frac{\phi(f, \mathbf{x}_{q_0} \rightarrow \mathbf{x}_{q_1})}{\phi(f, \mathbf{x}_{q_1} \rightarrow \mathbf{x}_{q_0})} \cdots \frac{\phi(f, \mathbf{x}_{q_{k-1}} \rightarrow \mathbf{x}_{q_k})}{\phi(f, \mathbf{x}_{q_k} \rightarrow \mathbf{x}_{q_{k-1}})} = 1,$$

by the symmetric cycle axiom since $p_k = q_k$ and $p_0 = q_0$. Furthermore, we know that $\alpha'_i \neq 0$ for all i , since all terms are non-zero by definition of connected component.

We then define

$$K'(\mathbf{x}_i, \mathbf{x}_j) = \begin{cases} \phi(f, \mathbf{x}_i \rightarrow \mathbf{x}_j) / \alpha'_i & , \text{ for } i \in [m] \text{ and } j \in [n] \setminus \{i\}. \\ |\phi(f, \mathbf{x}_i \rightarrow \mathbf{x}_j) / \alpha'_i| & , \text{ for } i = j \in [m]. \\ \phi(f, \mathbf{x}_j \rightarrow \mathbf{x}_i) / \alpha'_j & , \text{ for } i \in \{m+1, \dots, n\} \text{ and } j \in [m]. \\ 0 & , \text{ for } i, j \in \{m+1, \dots, n\}. \end{cases}$$

Prove that K' is a symmetric function. We first consider the case where both i and j belong to $[m]$.

If \mathbf{x}_i and \mathbf{x}_j are in the same connected component, by definition the reference point \mathbf{x}_r will be the same for \mathbf{x}_i and \mathbf{x}_j . If $\phi(f, \mathbf{x}_i \rightarrow \mathbf{x}_j) = 0$, by symmetric-zero axiom $\phi(f, \mathbf{x}_j \rightarrow \mathbf{x}_i) = 0$, and thus $K'(\mathbf{x}_i, \mathbf{x}_j) = K'(\mathbf{x}_j, \mathbf{x}_i) = 0$. If $\phi(f, \mathbf{x}_i \rightarrow \mathbf{x}_j) \neq 0$ and $\phi(f, \mathbf{x}_j \rightarrow \mathbf{x}_i) \neq 0$, without loss of generality, assume the path from \mathbf{x}_i to \mathbf{x}_r is p and the path from \mathbf{x}_j to \mathbf{x}_r is q , where path p has length k_1 and path q has length k_2 .

$$\begin{aligned} \frac{K'(\mathbf{x}_i, \mathbf{x}_j)}{K'(\mathbf{x}_j, \mathbf{x}_i)} &= \frac{\phi(f, \mathbf{x}_i \rightarrow \mathbf{x}_j) / \alpha'_i}{\phi(f, \mathbf{x}_j \rightarrow \mathbf{x}_i) / \alpha'_j} \\ &= \frac{\phi(f, \mathbf{x}_i \rightarrow \mathbf{x}_j) \cdot \phi(f, \mathbf{x}_j \rightarrow \mathbf{x}_{q_1}) \cdots \phi(f, \mathbf{x}_{q_{k_2}} \rightarrow \mathbf{x}_r) \cdot \phi(f, \mathbf{x}_r \rightarrow \mathbf{x}_{p_{k_1}}) \cdots \phi(f, \mathbf{x}_{p_1} \rightarrow \mathbf{x}_i)}{\phi(f, \mathbf{x}_j \rightarrow \mathbf{x}_i) \cdot \phi(f, \mathbf{x}_i \rightarrow \mathbf{x}_{p_1}) \cdots \phi(f, \mathbf{x}_{p_{k_1}} \rightarrow \mathbf{x}_r) \cdot \phi(f, \mathbf{x}_r \rightarrow \mathbf{x}_{q_{k_2}}) \cdots \phi(f, \mathbf{x}_{q_1} \rightarrow \mathbf{x}_j)} \\ &= 1, \end{aligned}$$

where the last equality is implied by the symmetric cycle axiom. Next, if \mathbf{x}_i and \mathbf{x}_j are not in the same connected component, there is no edge between \mathbf{x}_i and \mathbf{x}_j . It implies that either $\phi(f, \mathbf{x}_i \rightarrow \mathbf{x}_j) = 0$ or $\phi(f, \mathbf{x}_j \rightarrow \mathbf{x}_i) = 0$ by the definition of the graph. However, due to the symmetric zero axiom, we should have $\phi(f, \mathbf{x}_i \rightarrow \mathbf{x}_j) = \phi(f, \mathbf{x}_j \rightarrow \mathbf{x}_i) = 0$. Thus we have $K'(\mathbf{x}_i, \mathbf{x}_j) = K'(\mathbf{x}_j, \mathbf{x}_i) = 0$.

If i and j are not in the same connected component, it implies that at least one $K'(\mathbf{x}_i, \mathbf{x}_j)$ and $K'(\mathbf{x}_j, \mathbf{x}_i)$ should be zero by definition of the connected component. However, it implies $K'(\mathbf{x}_i, \mathbf{x}_j) = K'(\mathbf{x}_j, \mathbf{x}_i) = 0$ due to the symmetric zero axiom. Finally, if at least one of i, j is not in $[m]$, we have $K'(\mathbf{x}_i, \mathbf{x}_j) = K'(\mathbf{x}_j, \mathbf{x}_i)$ by the definition of K' .

Lastly, we consider the case either i or j belongs to $\{m + 1, \dots, n\}$. If $i \in \{m + 1, \dots, n\}$ and $j \in [m]$, we have

$$K'(\mathbf{x}_i, \mathbf{x}_j) = \phi(f, \mathbf{x}_j \rightarrow \mathbf{x}_i) / \alpha'_j = K'(\mathbf{x}_j, \mathbf{x}_i)$$

Similarly, the results hold for the case when $j \in \{m + 1, \dots, n\}$ and $i \in [m]$. If we have both i, j belong to $\{m + 1, \dots, n\}$, we have $K'(\mathbf{x}_i, \mathbf{x}_j) = K'(\mathbf{x}_j, \mathbf{x}_i) = 0$

Therefore, $K'(\mathbf{x}_i, \mathbf{x}_j) = K'(\mathbf{x}_j, \mathbf{x}_i)$ for any two training points $\mathbf{x}_i, \mathbf{x}_j$ (if $i = j$ this also trivially holds).

Prove K' is a continuous positive-definite kernel: Now, we have $\phi(f, \mathbf{x}_i \rightarrow \mathbf{x}_j) = \alpha'_i K'(\mathbf{x}_i, \mathbf{x}_j)$ for any two arbitrary training points $\mathbf{x}_i, \mathbf{x}_j$ for some symmetric kernel function K' satisfying $K'(\mathbf{x}_i, \mathbf{x}_i) \geq 0$ for all training samples \mathbf{x}_i .

Next, since the explanation further satisfies the continuity and irreducibility axioms for all kinds of training points, the kernel should be a continuous positive definite kernel by Mercer's theorem [63].

Prove the other direction: Assume that some $K : \mathbb{R}^d \times \mathbb{R}^d \mapsto \mathbb{R}$ is some continuous positive-definite kernel function and the explanation can be expressed as

$$\phi(f, \mathbf{x}_i \rightarrow \mathbf{x}_j) = \alpha_i K(\mathbf{x}_i, \mathbf{x}_j), \forall i, j \in [n].$$

Below we prove that it satisfies the continuity, self-explanation, symmetric zero, symmetric cycle, and irreducibility axioms.

First, it satisfies the continuity axiom since the kernel is continuous. Second, if $\phi(f, \mathbf{x}_i \rightarrow \mathbf{x}_i) = 0$ for some training point \mathbf{x}_i , we have $\alpha_i K(\mathbf{x}_i, \mathbf{x}_i) = 0$. This implies that either $\alpha_i = 0$ or $K(\mathbf{x}_i, \mathbf{x}_i) = 0$ for all $\mathbf{x} \in \mathbb{R}^d$ since it is a positive-definite kernel. Therefore, it satisfies the self-explanation axiom.

Third, we prove that it satisfies the symmetric zero axiom. Since we have $\phi(f, \mathbf{x}_i \rightarrow \mathbf{x}_i) \neq 0$, it implies $\alpha_i \neq 0$. Therefore if we have $\phi(f, \mathbf{x}_i \rightarrow \mathbf{x}_j) = 0$ for some \mathbf{x}_j , it implies $K(\mathbf{x}_i, \mathbf{x}_j) = 0$. Since the kernel is symmetric, it also implies $\phi(f, \mathbf{x}_j \rightarrow \mathbf{x}_i) = \alpha_j K(\mathbf{x}_j, \mathbf{x}_i) = 0$.

Next, we prove that it satisfies the symmetric zero axiom.

$$\begin{aligned} \prod_{i=1}^k \phi(f, \mathbf{x}_{t_i} \rightarrow \mathbf{x}_{t_{i+1}}) &= \prod_{i=1}^k \alpha_{t_i} K(\mathbf{x}_{t_i}, \mathbf{x}_{t_{i+1}}) \\ &= \prod_{i=1}^k \alpha_{t_{i+1}} K(\mathbf{x}_{t_{i+1}}, \mathbf{x}_{t_i}) \\ &= \prod_{i=1}^k \phi(f, \mathbf{x}_{t_{i+1}} \rightarrow \mathbf{x}_{t_i}), \end{aligned}$$

where we use the fact that K is a symmetric kernel in the third equation.

Finally, by Mercer theorem, it satisfies the irreducibility axiom. □

E.2 Proof of Proposition 8

Proof. We solve the following reparameterized objective as in Eqn.(5).

$$\hat{\alpha} = \operatorname{argmin}_{\alpha \in \mathbb{R}^n} \left\{ \frac{1}{n} \sum_{i=1}^n \mathcal{L} \left(\sum_{j=1}^n \alpha_j K(\mathbf{x}_i, \mathbf{x}_j), f(\mathbf{x}_i) \right) + \frac{\lambda}{2} \alpha^\top \mathbf{K} \alpha \right\}.$$

By the first-order optimality condition, we have

$$\frac{\partial}{\partial \alpha} \left(\frac{1}{n} \sum_{i=1}^n \mathcal{L} \left(\sum_{j=1}^n \alpha_j K(\mathbf{x}_i, \mathbf{x}_j), f(\mathbf{x}_i) \right) + \frac{\lambda}{2} \alpha^\top \mathbf{K} \alpha \right) \Big|_{\alpha=\hat{\alpha}} = \mathbf{0}$$

By the chain rule, we have

$$\frac{1}{n} \sum_{i=1}^n \mathcal{L}' \left(\sum_{j=1}^n \hat{\alpha}_j K(\mathbf{x}_i, \mathbf{x}_j), f(\mathbf{x}_i) \right) \mathbf{K} e_i + \lambda \mathbf{K} \hat{\alpha} = \mathbf{0},$$

where $e_i \in \mathbb{R}^{n \times 1}$ denotes the i^{th} unit vector and $\mathcal{L}' \left(\sum_{j=1}^n \hat{\alpha}_j K(\mathbf{x}_i, \mathbf{x}_j), f(\mathbf{x}_i) \right) \in \mathbb{R}$ is the partial derivative of \mathcal{L} with respect to its first input. Then we arrange the equation:

$$\mathbf{K} \left(\frac{1}{n} \sum_{i=1}^n \mathcal{L}' \left(\sum_{j=1}^n \hat{\alpha}_j K(\mathbf{x}_i, \mathbf{x}_j), f(\mathbf{x}_i) \right) e_i + \lambda \hat{\alpha} \right) = \mathbf{0}$$

Therefore, we must have $\frac{1}{n} \sum_{i=1}^n \mathcal{L}' \left(\sum_{j=1}^n \hat{\alpha}_j K(\mathbf{x}_i, \mathbf{x}_j), f(\mathbf{x}_i) \right) e_i + \lambda \hat{\alpha} \in \text{null}(\mathbf{K})$. It implies that

$$\hat{\alpha} \in \left\{ \frac{-1}{n\lambda} \sum_{i=1}^n \mathcal{L}' \left(\sum_{j=1}^n \hat{\alpha}_j K(\mathbf{x}_i, \mathbf{x}_j), f(\mathbf{x}_i) \right) e_i + \text{null}(\mathbf{K}) \right\}.$$

We note that $\sum_{j=1}^n \hat{\alpha}_j K(\mathbf{x}_i, \mathbf{x}_j) = (\mathbf{K} e_i)^\top \hat{\alpha} = e_i^\top (\mathbf{K} \hat{\alpha})$ is a constant for all alphas in the above solution set. Therefore, we have

$$\hat{\alpha} \in \{\alpha^* + \text{null}(\mathbf{K})\},$$

where $\alpha_i^* = -\frac{1}{n\lambda} \frac{\partial \mathcal{L}(\hat{f}_K(\mathbf{x}_i), f(\mathbf{x}_i))}{\partial \hat{f}_K(\mathbf{x}_i)}$ for all $i \in [n]$.

□

E.3 Proof of Proposition 9

Proof. Let $v \in \text{null}(\mathbf{K})$. We consider the norm of $f_v = \sum_{i=1}^n v_i K(x_i, \cdot)$:

$$\begin{aligned} \|f_v\|_{\mathcal{H}}^2 &= \langle f_v, f_v \rangle = \left\langle \sum_{i=1}^n v_i K(x_i, \cdot), \sum_{i=1}^n v_i K(\cdot, x_i) \right\rangle \quad (\text{ kernels are symmetric to its inputs}) \\ &= \sum_{i=1}^n v_i \langle K(x_i, \cdot), \sum_{i=1}^n v_i K(\cdot, x_i) \rangle \\ &= v^\top \mathbf{K} v \\ &= 0 \quad (\mathbf{K} v = \mathbf{0}), \end{aligned}$$

which implies that $f_v(x) = 0$ for all $x \in \mathbb{R}^d$.

□

E.4 Proof of Corollary 12

By plugging the kernel function $K_{LL}(\mathbf{x}, \mathbf{z}) = \langle \Phi_{\theta_1}(\mathbf{x}), \Phi_{\theta_1}(\mathbf{z}) \rangle, \forall \mathbf{x}, \mathbf{z} \in \mathbb{R}^d$ to Proposition 8, we have

$$\hat{f}_K(\cdot) = \sum_{i=1}^n \alpha_i^* K_{LL}(\mathbf{x}_i, \cdot), \quad \text{with } \alpha_i^* = -\frac{1}{n\lambda} \frac{\partial \mathcal{L}(\hat{f}_K(\mathbf{x}_i), f(\mathbf{x}_i))}{\partial \hat{f}_K(\mathbf{x}_i)}.$$